

Lidar monitoring of regions of intense backscatter with poorly defined boundaries

Vladimir A. Kovalev,* Alexander Petkov, Cyle Wold, and Wei Min Hao

United States Forest Service, RMRS, Fire Sciences Laboratory, 5775 Highway 10 West, Missoula, Montana, 59808, USA

*Corresponding author: vkovalev@fs.fed.us

Received 31 August 2010; accepted 7 November 2010;
posted 19 November 2010 (Doc. ID 134285); published 27 December 2010

The upper height of a region of intense backscatter with a poorly defined boundary between this region and a region of clear air above it is found as the maximal height where aerosol heterogeneity is detectable, that is, where it can be discriminated from noise. The theoretical basis behind the retrieval technique and the corresponding lidar-data-processing procedures are discussed. We also show how such a technique can be applied to one-directional measurements. Examples of typical results obtained with a scanning lidar in smoke-polluted atmospheres and experimental data obtained in an urban atmosphere with a vertically pointing lidar are presented. © 2010 Optical Society of America

OCIS codes: 280.3640, 290.1350, 290.2200.

1. Introduction

There is no commonly accepted technique for remote monitoring of the locations and temporal and spatial changes of regions of increased backscatter with poorly defined boundaries, such as those that are found in dispersed smoke plumes originating in wildfires, dust clouds, or aerosol clouds created by volcanic eruptions.

To monitor the behavior of intense backscatter regions in the atmosphere, lidar is the most appropriate tool. In principle, lidar can easily detect the boundary between different atmospheric layers and discriminate the regions with high levels of backscatter from the regions of clear atmosphere. Well-defined heterogeneous areas, such as the atmospheric boundary layer or clouds, can be identified through the visual inspection of the lidar scan and is a trivial matter [1]. However, the identification of the exact location of the boundary of a heterogeneous structure becomes a significant challenge when the boundary is not well defined. Such a situation is typical, for example, for smoke layers and plumes where the dispersion processes create a

continuous transition zone between the intense backscatter region and clear air. The smoke plume density, its concentrations, the levels of the heterogeneity, and the smoke dispersion are extremely variable and depend heavily on the distance from the smoke plume source.

The absence of unique criteria for determining the boundary between the increased-backscatter and clear-air areas when it is not well defined is the principal issue when using any range-resolved remote sensing technique. This challenge is a general problem rather than a problem of remote-sensing methodology. No standard definition of such a boundary exists. When determining the boundaries of the aerosol formation, generally, some relative rather than absolute characteristics are used. For example, when using a gradient method, one can select the boundary location as the range where the examined parameter of interest (e.g., the derivative of the square-range-corrected lidar signal) is a maximum or decreases from the maximum value down to a fixed, user-defined level [2]. However, there is no way to establish a standard value for this level, which would be acceptable for all cases of atmospheric searching. Similarly, the use of the wavelet technique requires the selection of concrete parameters, and this is a significant challenge when a region of intense backscatter

with a poorly defined boundary is examined [3]. In this study, an alternative approach to this issue is considered.

2. Methodology

The lidar signal, $P_{\Sigma}(r)$, recorded at the range r , is the sum of the range-dependent backscatter signal, $P(r)$ and the range-independent offset, B , the background component of the lidar signal and the electronic offset:

$$P_{\Sigma}(r) = P(r) + B. \quad (1)$$

This signal is transformed in the auxiliary function $Y(x)$, defined as [4]

$$Y(x) = P_{\Sigma}(x)x = [P(x) + B]x, \quad (2)$$

where $x = r^2$ is the new independent variable. In the current study, we apply the simplest form of the transformation, which does not require the use of the molecular profile of the searched atmosphere. The sliding derivative of this function, dY/dx , is calculated, and the intercept point of each local slope fit of the function with the vertical axis is found and normalized. The intercept function versus x is found as

$$Y_0(x) = Y(x) - \frac{dY}{dx}x. \quad (3)$$

By using the intercept function instead of dY/dx , the determination of the systematic offset, B , in the lidar signal [Eq. (1)] can be avoided. The retrieval technique that is used here for processing the signals of both scanning and one-directional lidar is based on determining the normalized intercept function [4]. The normalized intercept function is defined as

$$Y_{0,\text{norm}}(x) = \frac{Y_0(x)}{x + \varepsilon x_{\text{max}}}, \quad (4)$$

where x_{max} is the maximum value of the variable x over the selected range and ε is a positive nonzero constant, whose value can range from 0.02–0.05. The selection of the numerical value for ε is not critical. The component $\varepsilon x_{\text{max}}$ in the denominator of the equation is included only to suppress the excessive increase of $Y_{0,\text{norm}}(x)$ in the region of small x , which, for our task, is not the region of interest. Note also that the numerical differentiation in Eq. (3) is made with a constant step, $\Delta r = r_{i+1} - r_i = \text{const.}$, rather than a constant Δx . Under such a condition, the step Δx is variable, that is,

$$\Delta x = r_{i+1}^2 - r_i^2 = \Delta r^2 \left(1 + \frac{2r_i}{\Delta r} \right). \quad (5)$$

In this paper, we restrict our analysis to the determination of the maximum heights of the regions of the increased backscatter; the determination of the minimum heights, especially in a multilayering atmo-

sphere, is a much more complicated task and requires separate consideration.

A. Determination of the Maximal Height of the Region of Increased Backscatter Using Scanning Lidar

Consider the case where lidar scanning is performed in a fixed azimuthal direction, θ , using N_{φ} slope directions selected within the angular sector from φ_{min} to φ_{max} and with the stepped angular resolution of $\Delta\varphi$; that is, $\varphi_1 = \varphi_{\text{min}}$, $\varphi_2 = \varphi_{\text{min}} + \Delta\varphi, \dots$, $\varphi_i = \varphi_{\text{min}} + (i-1)\Delta\varphi, \dots$, and $\varphi_N = \varphi_{\text{max}}$. The recorded signals, measured within the range from r_{min} to r_{max} , are transformed into the corresponding set of the normalized functions, $Y_{0,\text{norm}}(h)$, versus height, h ; these functions are calculated within the altitude range from h_{min} to h_{max} with the selected height resolution, Δh ; that is, $h_1 = h_{\text{min}}$, $h_2 = h_{\text{min}} + \Delta h, \dots$, $h_j = h_{\text{min}} + (j-1)\Delta h, \dots$, and $h_M = h_{\text{max}}$; M is the number of heights within the selected interval $[h_{\text{min}}, h_{\text{max}}]$.

To locate the maximum height of the region of increased backscatter, the absolute values of the normalized intercept function versus height for each slope direction φ_i and each h_j within the altitude range from h_{min} to h_{max} , are calculated:

$$f_{i,j} = |Y_{0,\text{norm}}(\varphi_i, h_j)|. \quad (6)$$

Thus, for our calculations we define the matrix \mathbf{F}_{φ} , with matrix elements $f_{i,j} \in (N_{\varphi}, M)$; that is, $\mathbf{F}_{\varphi} = [f_{i,j}]_{N_{\varphi} \times M}$. The maximum matrix element, $f_{\text{max}} = \max[f_{i,j}]_{N_{\varphi} \times M}$, is determined and the matrix is normalized:

$$\mathbf{R}_{\varphi} = \frac{1}{f_{\text{max}}} \mathbf{F}_{\varphi}. \quad (7)$$

The elements of the matrix, $r_{i,j} = R(\varphi_i, h_j)$, which are used for determining the areas of the smoke plume, can vary within the range $0 \leq r_{i,j} \leq 1$, with areas approaching $r_{i,j} = 1$ having the greatest heterogeneity.

In our original study [4], the local ‘‘heterogeneity event’’ defined in two-dimensional space (i, j) was implemented. The event was considered as being true at the locations where the elements $r_{i,j}$ of the matrix \mathbf{F}_{φ} reach some established, user-defined level, $\chi < 1$. In other words, we supposed that the atmospheric heterogeneity in the cell (i, j) , exists if the element, $r_{i,j} \geq \chi$; in the study [4], the user-defined constant χ was selected within the range from 0.15 to 0.3. Some modification in selecting χ was considered in [5].

To clarify the modified methodology for the determination of the maximal height of the smoke-polluted area and the principle for the selection of χ in this study, let us consider typical experimental data. The data were obtained by a scanning lidar in the vicinity of the Kootenai Creek Fire near Missoula, Montana, USA in 2009. The wildfire occurred in a wild mountainous area from which the smoke plume spread in an easterly direction across the valley where the lidar was located. The height of

the lidar site was approximately 900 m below the height of the wildfire area. The schematic of the scanning lidar setup is shown in Fig. 1. Lidar vertical scans were made along 23 azimuthal directions, from $\theta = 45^\circ$ to $\theta = 155^\circ$, with an angular increment $\Delta\theta = 5^\circ$. Thus, each scan was used to obtain a vertical cross-section of attenuated backscatter in the corresponding azimuthal direction.

In Figs. 2–5, we clarify the details of our data-processing methodology using the results obtained on 27 August 2009. The vertical scan analyzed below was made at the azimuthal direction, $\theta = 55^\circ$, within the vertical angular sector from $\varphi_{\min} = 10^\circ$ to $\varphi_{\max} = 60^\circ$; the total number of slope directions is $N_\varphi = 28$. In Fig. 2, the corresponding 28 functions, $R(\varphi_i, h_j)$, are shown as the gray curves, with the thick black curve representing the resulting heterogeneity function, $R_{\theta, \max}(h)$, defined for each altitude as

$$R_{\theta, \max}(h) = \max[R(\varphi_1, h), R(\varphi_2, h), \dots, R(\varphi_N, h)]. \quad (8)$$

To determine the maximum height of the smoke-polluted region, the parameter, χ , can be selected and compared to $R_{\theta, \max}(h)$. The maximum smoke plume height, $h_{\text{sm}, \max}$, can be found as the maximum height where $R_{\theta, \max}(h) = \chi$. The main issue of such an approach is the rational selection of χ . In the case of a poorly defined boundary, the retrieved height of the smoke plume strongly depends on the selected χ . This observation is illustrated in Fig. 3, where the $R_{\theta, \max}(h)$ shown in Fig. 2 is analyzed. One can see that selecting different χ yields different heights of interest, $h_{\text{sm}, \max}$. For example, changing χ from 0.1 to 0.15 decreases the retrieved height $h_{\text{sm}, \max}$ from 4581 to 3078 m.

Analyzing possible retrieval techniques, we concluded that the optimal solution could be achieved by taking advantage of the principles used for determining the cloud base height when the ceiling has no well-defined lower boundary. In such a case, the cloud base height is considered as the lowest level

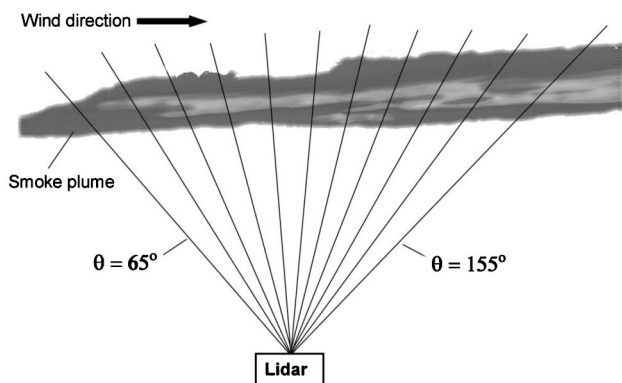


Fig. 1. Schematic of data collection with a vertically scanning lidar during the Kootenai Creek Fire in Montana in July and August 2009. (The azimuthal sector $45^\circ - 65^\circ$, which overlaps the wildfire site, is not shown in this figure.)

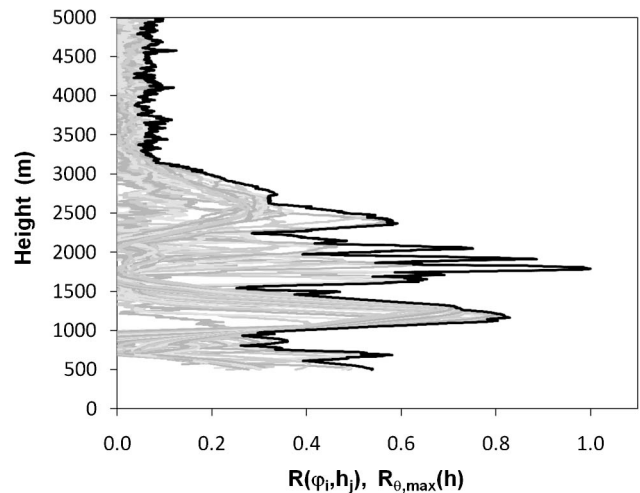


Fig. 2. Example of data obtained by a scanning lidar at the wavelength of 1064 nm in the smoke-polluted atmosphere in the vicinity of Missoula, Montana. The gray curves represent the set of 28 functions, $R(\varphi_i, h_j)$. The resulting heterogeneity function, $R_{\theta, \max}(h)$, is shown as the thick black curve.

of the atmosphere where cloud properties are detectable [6]. In our study, the analogous definition is used for determining the maximum smoke plume height. Particularly, the upper smoke plume boundary height, $h_{\text{sm}, \max}$, can be defined as the maximum height where smoke plume aerosols are detectable in the presence of the noise component in the examined function. This approach requires reliably distinguishing the $r_{i,j}$ increases caused by the presence of the actual smoke plume heterogeneity from that of random noise fluctuations.

To apply the above definition in the smoke plume measurements, the following methodology was chosen. Using the retrieved functions, $R_{\theta, \max}(h)$ (Fig. 2), the atmospheric heterogeneity height indicator (AHHI) for this azimuth θ is determined. The AHHI

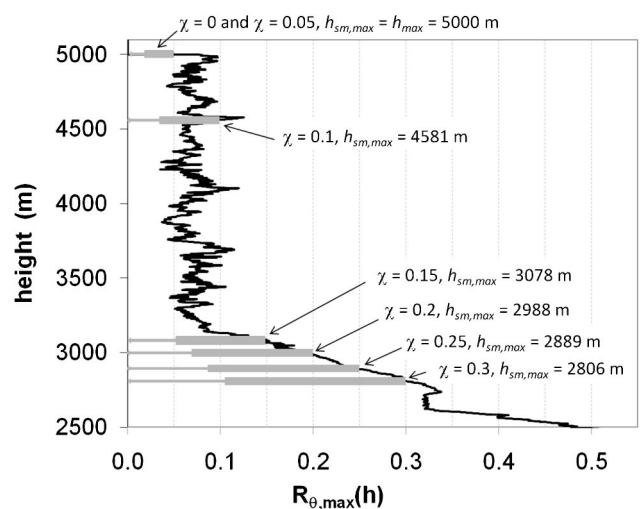


Fig. 3. Black curve is the same heterogeneity function, $R_{\theta, \max}(h)$, as in Fig. 2, and the gray blocks illustrate the dependence of the retrieved smoke plume height, $h_{\text{sm}, \max}$, on the selected χ .

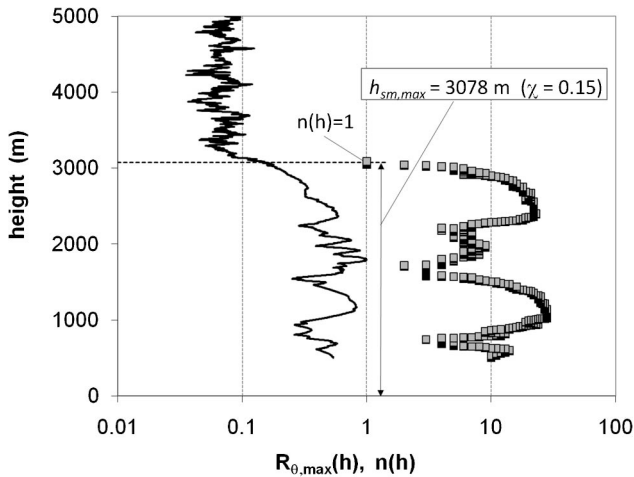


Fig. 4. Black-gray squares show the AHHI derived with $\chi_{opt} = 0.15$. The maximal height, where the minimal number of the heterogeneity events exceeds zero [that is, $n(h) = 1$], is $h_{sm, \max} = 3078$ m. The thick black curve is the function $R_{\theta, \max}(h)$, the same as in Figs. 2 and 3.

is a histogram that shows the total number of heterogeneity events, $n(h)$, defined by scanning lidar at the consecutive height intervals for the selected χ [4]. The concept of the AHHI histogram is explained in Fig. 4. The thick black curve on the left side of the figure is the function $R_{\theta, \max}(h)$, the same as in Figs. 2 and 3. The AHHI derived with the level $\chi = 0.15$, is shown as black-gray squares. The maximal height, where the minimal number of the heterogeneity events exceeds zero [$n(h) = 1$], is $h_{sm, \max} = 3078$ m. Note also that a maximum number of heterogeneity events was fixed over the altitude range 1000 m–1150 m ($n = 28$) and 2350–2550 m ($n = 22$), so that two separate layers at different heights can be discriminated with the AHHI.

Using such AHHI histograms, one can determine the maximal heights of the area with the increased heterogeneity for different χ . In our calculations, we utilize the consecutive values of χ with the fixed step $\Delta\chi$; that is, $\chi_0 = 0$, $\chi_1 = \Delta\chi$, $\chi_2 = 2\Delta\chi, \dots$, and $\chi_k = k\Delta\chi, \dots$. For each discrete χ , we build the AHHI and determine the corresponding maximum height, $h_{sm, \max}(\chi)$, that is, the maximum height where the number of heterogeneity events, $n(h)$, is a nonzero integer value.

The height of interest, $h_{sm, \max}$, is determined using the minimal value of χ that allows reliable discriminating of the smoke plume heterogeneity from the noise component. Figure 5 illustrates the basic principle for the determination of optimal level, χ_{opt} , which provides the most likely smoke plume height, $h_{sm, \max}(\chi_{opt})$. The methodology of determining χ_{opt} and the corresponding $h_{sm, \max}(\chi_{opt})$ is as follows. Initially, the level $\chi_0 = 0$ is selected. Because of the presence of nonzero instrumental noise, the height, $h_{sm, \max}(\chi_0)$, determined from AHHI as the maximal height where $n(h) > 0$, will be equal to the selected h_{max} . In our case, $h_{sm, \max}(\chi_0) = h_{max} = 5000$ m

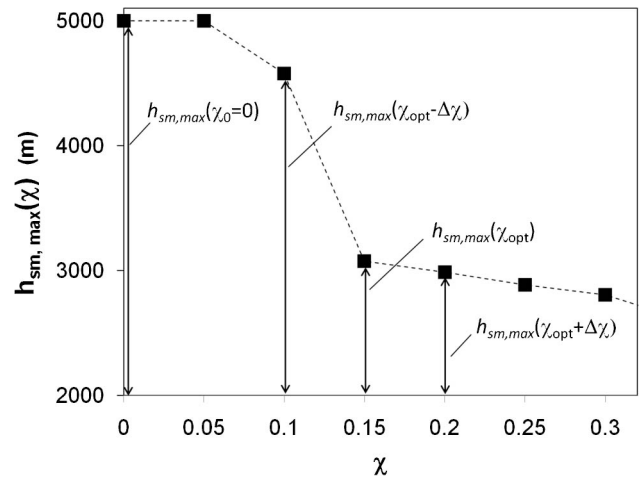


Fig. 5. Dependence of the retrieved height, $h_{sm, \max}$, on the selected χ for the heterogeneity function, $R_{\theta, \max}(h)$, shown in Figs. 2–4.

(Fig. 3). Then the next level, $\chi_1 = \Delta\chi = 0.05$, is analyzed. One can see in Fig. 5 that this level does not change the initial height, $h_{sm, \max} = 5000$ m, that is, the level $\chi_1 = 0.05$ is still below the interfering noise. Selecting then the larger levels, equal to $\chi_2 = 0.1$ and $\chi_3 = 0.15$, we plot the set of corresponding AHHI and for each χ determine the maximal heights where $n(h) > 0$, that is, the heights $h_{sm, \max}(\chi_2)$ and $h_{sm, \max}(\chi_3)$ (Fig. 5). The goal of this operation is to establish when the erroneous heterogeneity events created by noise become below the level of discrimination, χ , so that the actual $h_{sm, \max}$ can be found.

The determination of the optimal level, χ_{opt} , and the corresponding height of interest, $h_{sm, \max}(\chi_{opt})$, is based on the calculation of the differences between the adjacent heights $h_{sm, \max}(\chi_k)$ and $h_{sm, \max}(\chi_{k+1})$. The established value of χ_{opt} should meet two conditions. First, the difference $h_{sm, \max}(\chi_{opt} - \Delta\chi) - h_{sm, \max}(\chi_{opt})$ should be maximal. Second, the next consecutive increase of χ , that is, selection of χ equal to $\chi_{opt} + \Delta\chi$, then $\chi_{opt} + 2\Delta\chi$ should result in a slow decrease in the corresponding $h_{sm, \max}(\chi)$.

In our case, the decrease from $\chi = 0.1$ to 0.15 results in the largest decrease of $h_{sm, \max}(\chi)$ from 4581 to 3078 m (Figs. 3 and 5). The next consecutive increase of χ from 0.15 to 0.2, then from 0.2 to 0.25, do not reduce the extracted $h_{sm, \max}(\chi)$ significantly; the difference between any pair of the consecutive maximum heights, $h_{sm, \max}(\chi_k)$ and $h_{sm, \max}(\chi_{k+1})$, is less than 100 m, that is, $\sim 3\%$ relative to the fixed smoke plume heights.

Thus, the application of this method to our data yields the optimal level, $\chi_{opt} = 0.15$ and the corresponding $h_{sm, \max}(\chi_{opt}) = 3078$ m. It is worth also worth mentioning that to avoid significant underestimating the smoke plume maximum height, the χ_{opt} should be small, presumably within the range of 0.1–0.2. This requirement puts reasonable restrictions on the level of the interfering noise.

Two typical situations can be met when determining χ_{opt} . If the smoke plume has an upper boundary

with no local layering in its vicinity, both requirements are met: the systematic difference between the heights, determined with the consecutive levels, $\chi_{\text{opt}}, \chi_{\text{opt}} + \Delta\chi, \dots, \chi_{\text{opt}} + 2\Delta\chi, \dots$, is small, whereas the difference between the heights, determined with the level, χ_{opt} and the previous level, $\chi_{\text{opt}} - \Delta\chi$, is maximum.

The situation may be different when the multiple layering with different levels of backscattering exists in the area of the upper boundary of the smoke plume. In this case, the second condition may be not met. That is, the maximum difference between heights $h_{\text{sm,max}}(\chi_{\text{opt}})$ and $h_{\text{sm,max}}(\chi_{\text{opt}} - \Delta\chi)$ takes place whereas the difference between $h_{\text{sm,max}}(\chi_{\text{opt}})$ and $h_{\text{sm,max}}(\chi_{\text{opt}} + \Delta\chi)$ is significantly larger than the difference between $h_{\text{sm,max}}(\chi_{\text{opt}} + \Delta\chi)$ and $h_{\text{sm,max}}(\chi_{\text{opt}} + 2\Delta\chi)$. As shown below, this observation is used to obtain supplementary information about the boundaries of the examined smoke plume.

The above technique was used for processing lidar data obtained during the Kootenai Creek Fire in July and August 2009. To obtain information on the spread of the smoke plume, the vertical scans were performed under the different azimuthal directions, as shown in Fig. 1. From each vertical scan, the maximum smoke plume heights were determined using dependencies like those shown in Figs. 2–5. An example of the retrieved heights, obtained on 27 August 2009, from 12:09 to 12:27 local time, is shown in Fig. 6. We determined two consequent heights, $h_{\text{sm,max}}(\chi_{\text{opt}})$ and $h_{\text{sm,max}}(\chi_{\text{opt}} + \Delta\chi)$ rather than the first only. These heights for the examined 23 azimuthal directions, from 45° to 155° , are shown as the filled and empty triangles, respectively. It follows from the figure that the maximal heights of the smoke plume slowly decrease as the smoke moves away from the site of its origin source. The enlarged difference between the two consequent heights, for example, along the azimuthal directions 130° and

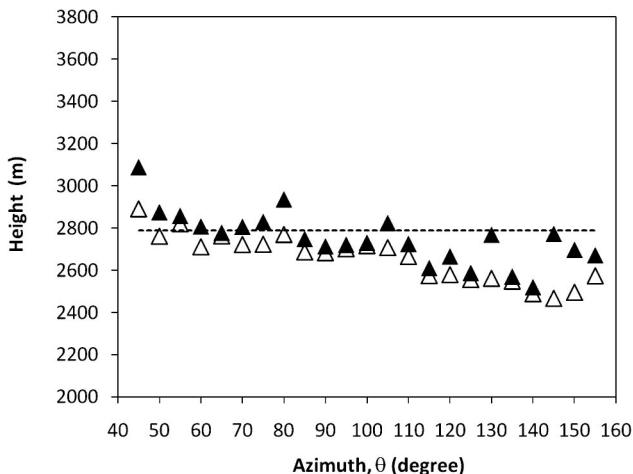


Fig. 6. Maximum heights of the smoke plume determined at different azimuthal directions measured in the vicinity of the Kootenai Creek Fire on 27 August 2009 during the period from 12:09 to 12:27. The horizontal dashed line indicates the smoke plume height determined from airborne measurements.

145° , indicates that the upper smoke boundaries here are not well defined. The horizontal dashed line indicates the smoke plume height determined from airborne measurements of aerosol concentration downwind of the Kootenai Creek fire [7].

B. Determination of the Maximal Height of the Intense Backscatter Area Using the One-Directional Pointing Mode

In this section, we consider the essentials of our technique for processing the data of vertically pointed lidar. This simplified technique, which adapts the principles discussed in the previous section, can be used for monitoring temporal changes that occur in urban atmospheres when the use of scanning mode is impossible due to the absence of the open space for scanning. Furthermore, in urban conditions, lidar scanning is usually not permitted due to eye safety regulations, and therefore, the lidar typically operates in the vertical direction.

We will discuss here the specifics of the one-directional lidar measurement results obtained in the CalNex-LA 2010 experiment [8]. The project was focused on studying the pollution sources in the Los Angeles urban area. We will consider here only essentials of our retrieval technique for determining the temporal changes in the heights of increased backscatter with a vertically pointed lidar, not analyzing the atmospheric situations, and not discussing the meteorological processes that influenced these temporal changes in the boundary layer during the experiment.

As with the multiangle mode, the determination of the maximum height of the polluted air is made by calculating the absolute value of the normalized intercept function versus height. The only difference is that the function is determined for the consecutive temporal periods, t ; that is, here the elements of matrix

$$f_{i,j}^* = |Y_{0,\text{norm}}(t_i, h_j)|, \quad (9)$$

are found, where $Y_{0,\text{norm}}$ is determined using Eq. (4).

The lidar measurement at the wavelength 1064 nm was performed daily, from 8:00 to 17:30. A one-minute average (1800 pulses) was recorded every 15 min from 20 May to 31 May 2010. In Fig. 7, the maximal heights of the polluted air measured during 24 May 2010, were determined in a similar manner as in Fig. 6. The empty diamonds show the heights obtained with $\chi_{\text{opt}} = 0.1$, and the filled diamonds show the heights obtained with $\chi = \chi_{\text{opt}} + \Delta\chi = 0.15$. Note that the increased difference between heights $h_{\text{sm,max}}(\chi_{\text{opt}})$ and $h_{\text{sm,max}}(\chi_{\text{opt}} + \Delta\chi)$, that is, the blurred and poorly defined boundary between the polluted and clear air above, occurred mostly in the morning hours. These heights tend to increase during the day except for the period from 13:30 to 15:00. The heights of the maximum heterogeneity, determined with $\chi = 0.9$ (the filled circles), clearly reveal a typical daytime increase of the maximum height of the polluted area from

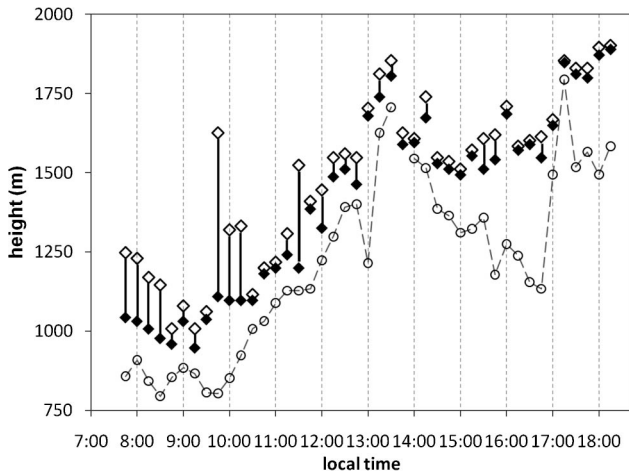


Fig. 7. Maximal heights of the polluted air obtained for different χ during the CalNex-LA experiment in Pasadena, Calif., on 24 May 2010. The empty diamonds show the heights obtained with $\chi_{\text{opt}} = 0.1$, the filled diamonds show the heights obtained with $\chi = \chi_{\text{opt}} + \Delta\chi = 0.15$, and the vertical lines show the cases of the increased difference between the heights, $h_{\text{sm,max}}(\chi_{\text{opt}})$ and $h_{\text{sm,max}}(\chi_{\text{opt}} + \Delta\chi)$. The heights of the maximum heterogeneity ($\chi = 0.9$) are shown as empty circles.

approximately, 10:00 till 13:30 local time and its decrease from 14:00 to 16:45. However, starting at 17:00, these heights also increase. This effect is caused by the appearance of the detached aerosol layers close to the top of the planetary boundary layer, which are clearly seen in the corresponding square-range-corrected signals (Fig. 8). This effect, which occurs typically during the afternoon hours, is well known [9,10]. When determining the boundary layer height, such detached layers lead to ambiguity in the choice of the “relevant” minimum in the gradient that corresponds to the height. There are different ways for avoiding this challenge. For example, one can either combine the variance and the gradient methods [11], or apply the gradient method

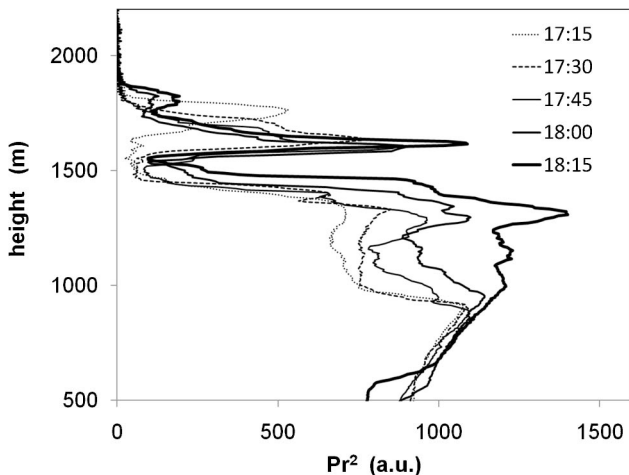


Fig. 8. Range-corrected signals, $P(r)r^2$, versus height obtained on 24 May 2010 from 17:15 to 18:15. The detached aerosol layers close to the top of the boundary layer, at the heights $\sim 1550 - 1850$ m, are clearly seen.

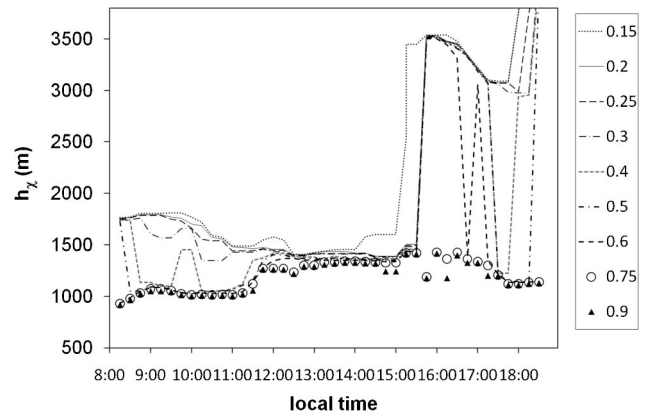


Fig. 9. χ -isoclinic lines obtained on 25 May 2010 for the set of fixed χ . The values of χ are shown in the legend.

with the requirement of minimum continuity [12]. We believe that the use of the data processing principles described in this paper can provide useful information for analyses of processes in the boundary layer.

In the results presented in Fig. 7, the same value of $\chi_{\text{opt}} = 0.1$ was obtained during the whole day. Another atmospheric situation was monitored the following day, on 25 May 2010. The atmospheric optical conditions during that day were extremely variable, so that the retrieved χ_{opt} varied from 0.05 to 0.5, making such retrieved heights incomparable. For this situation, the processing technique can be used that analyzes the behavior of the χ -isoclinic lines, that is, the temporal behavior of the heights extracted with fixed χ . Obviously, in the areas of well-defined boundaries, the adjacent values of χ create isoclinic lines that are close to each other. In contrast, large differences in the retrieved heights obtained for adjacent χ show polluted areas with poorly defined boundaries. In Fig. 9, the isoclinic lines for 25 May 2010 are shown. During that day, a relatively well-defined boundary existed: (a) at the heights of 1000–1100 m and between 1450 and 1800 m for the period from 8:45 to 11:15, (b) at the heights 1350–1450 m for the period from 12:00 to 15:00, and (c) at the heights 3100–3500 m for the period from 15:45 to 17:30 (χ from 0.2 to 0.5). Accordingly, the transition periods took place from 11:15 to 12:00 and from 15:00 to 15:45, respectively. Note that during the whole day, the heights of maximal heterogeneity, obtained here with $\chi = 0.75$ and $\chi = 0.9$, change within the relatively restricted range, from approximately 1000 to 1400 m, having maximal values from 12:00 to 17:00, and the minimal in the morning, before noon, and after 17:00.

3. Summary

Regions of increased backscattering, such as the dispersed smoke plumes originated by wildfires, often have poorly defined boundaries and extremely large ranging backscatter coefficients within the polluted area. This significantly impedes the determination of temporal and spatial changes of these formations with lidar. The result of the lidar measurement of

such an important parameter as the maximum height of an area of increased backscatter will depend on the user definition of such a boundary, levels of backscattering within the formation, and the relative level of noise in measurement data. Neither commonly accepted methodology of such measurements exists for both one-directional and multiangle scanning lidar.

The transformation of the lidar signal, proposed in this study, significantly simplifies the determination of the parameters of interest, and it can be utilized both in the scanning and one-directional mode. The implementation of the definition of the upper boundary height of the region of increased backscatter as the maximal height where the aerosol heterogeneity is detectable provides the maximal sensitivity for the aerosol particulate detection in the presence of signal noise.

The application of different levels of χ for determining the maximum heights of the region of increased backscatter allows establishing the heights of maximum heterogeneity and discriminating the areas both with well and poorly defined boundaries. The measurement methodology is simple and robust.

It follows from this study that the retrieved parameters of interest for the regions of increased backscatter are much more informative if these data are analyzed in the two-dimensional form, for example, as the height–azimuthal dependence for the scanning lidar and as the height–time dependence for the vertically pointed lidar.

References

1. D. I. Cooper and W. E. Eichinger, "Structure of the atmosphere in an urban planetary boundary layer from lidar and radiosonde observations," *J. Geophys. Res.* **99**, 22937–22948 (1994).
2. L. Menut, C. Flamant, J. Pelon, and P. H. Flamant, "Urban boundary-layer height determination from lidar measurements over the Paris area," *Appl. Opt.* **38**, 945–954 (1999).
3. I. M. Brooks, "Finding boundary layer top: Application of a wavelet covariance transform to lidar backscatter profiles," *J. Atmos. Oceanic Technol.* **20**, 1092–1105 (2003).
4. V. A. Kovalev, A. Petkov, C. Wold, S. Urbanski, and W. M. Hao, "Determination of smoke plume and layer heights using scanning lidar data," *Appl. Opt.* **48**, 5287–5294 (2009).
5. V. Kovalev, A. Petkov, C. Wold, and W. M. Hao, "Determination of the smoke-plume heights with scanning lidar using alternative functions for establishing the atmospheric heterogeneity locations," in *Proceedings of the 25th International Laser Radar Conference (IAO SB RAS, 2010)*, pp. 71–74.
6. <http://www.arm.gov/measurements/cloudbase> Website of The ARM Climate Research Facility, U.S. Department of Energy.
7. S. Urbanski, V. Kovalev, W. M. Hao, C. Wold, and A. Petkov, "Lidar and airborne investigation of smoke plume characteristics: Kootenai Creek Fire case study," in *Proceedings of the 25th International Laser Radar Conference (IAO SB RAS, 2010)*, pp. 1051–1054.
8. <http://www.esrl.noaa.gov/csd/calnex/whitepaper.pdf>
9. B. Hennemuth and A. Lammert, "Determination of the atmospheric boundary layer height from radiosonde and lidar backscatter," *Bound.-Layer Meteorol.* **120**, 181–200 (2006).
10. K. J. Davis, N. Gamage, C. R. Hagelberg, C. Kiemle, D. H. Lenschow, and P. P. Sullivan, "An objective method for deriving atmospheric structure from airborne lidar observations," *J. Atm. Oceanic Technol.* **17**, 1455–1468 (2000).
11. A. Lammert and J. Bösenberg, "Determination of the convective boundary-layer height with laser remote sensing," *Bound.-Layer Meteorol.* **119**, 159–170 (2006).
12. V. Mitev, R. Matthey, and V. Makarov, "Compact micro-pulse backscatter lidar and examples of measurements in the planetary boundary layer," *Rom. J. Phys.* (to be published).